

# Iterative Image Reconstruction for Helical X-ray CT Baggage Scans

---

Sherman Kisner<sup>1</sup>, Charles Bouman<sup>1</sup>, Ken Sauer<sup>2</sup>,  
Sondre Skatter<sup>3</sup>, Matthew Merzbacher<sup>3</sup>

<sup>1</sup> School of Electrical and Computer Engineering, Purdue University

<sup>2</sup> Department of Electrical Engineering, University of Notre Dame

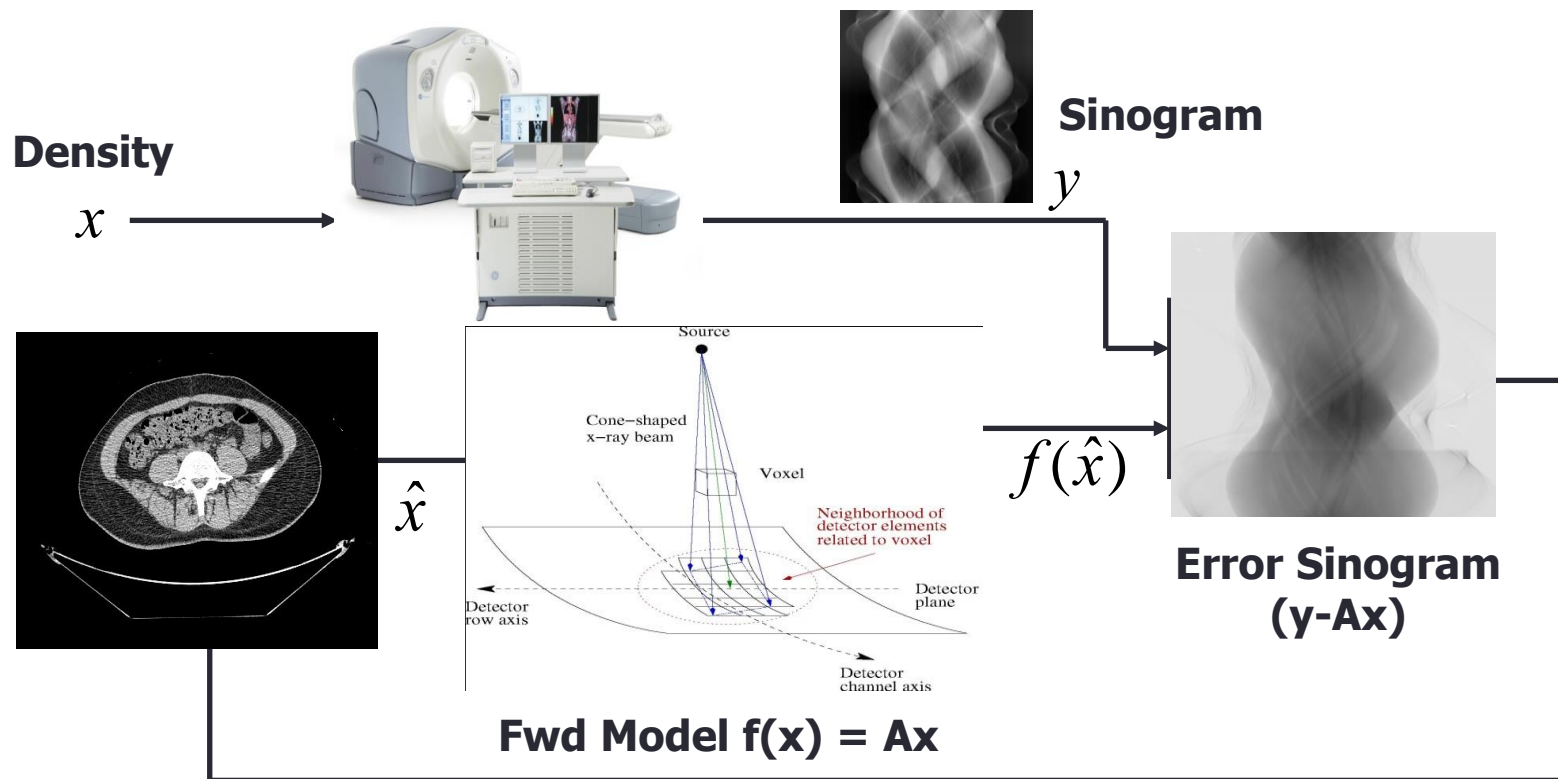
<sup>3</sup> Morpho Detection, Inc.



**ALERT**  
AWARENESS AND LOCALIZATION  
OF EXPLOSIVES-RELATED THREATS

This work was supported by the DHS ALERT Center of Excellence. Special thanks to Carl Crawford, John Beaty, and Michael Silevitch.

# Model-Based Iterative Reconstruction

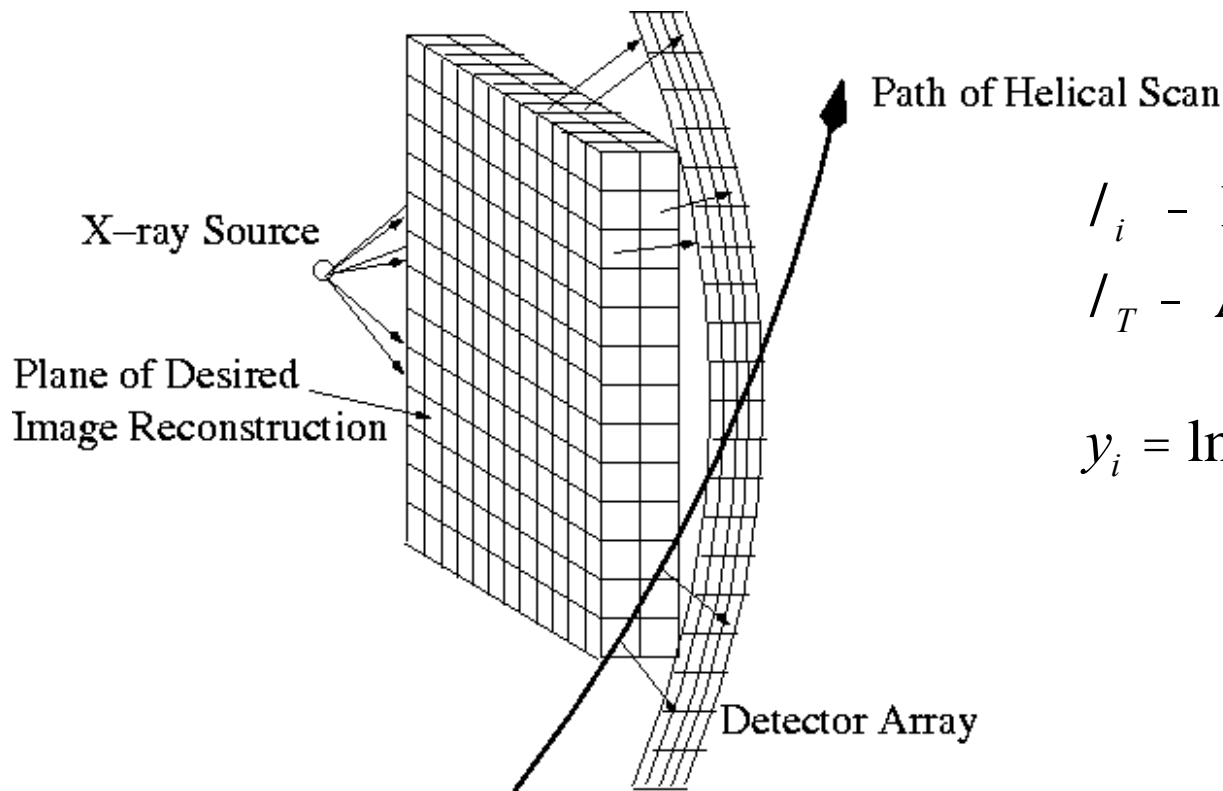


**Cost Function**

$$\hat{x}_{MAP} = \arg \max_{x \geq 0} \left\{ \log p(y | x) + \log p(x) \right\}$$

$$= \arg \min_{x \geq 0} \left\{ \frac{1}{2} (y - Ax)^T D (y - Ax) + U(x) \right\}$$

# Scanner forward model



$I_i$  - Photon count at detector

$I_T$  - Air calibration scan

$$y_i = \ln\left(\frac{I_T}{I_i}\right) - \text{Attenuation}$$

- Need to accurately and efficiently model the:
  - 3D forward projection geometry
  - Detector and source geometry and physics
  - Noise and distortion

# Data model

- Taylor expansion of Poisson log likelihood produces

$$\log p(\mathbf{y} | \mathbf{x}) \approx -\frac{1}{2} (\mathbf{y} - \mathbf{Ax})^t \mathbf{D} (\mathbf{y} - \mathbf{Ax})$$

- $y_i = -\log(I_i / I_{T,i})$  where  $I_i$  and  $I_{T,i}$  are measured photon counts

- Matrix  $A$  is a linear projection operator

- $D$  is a diagonal noise weighting matrix

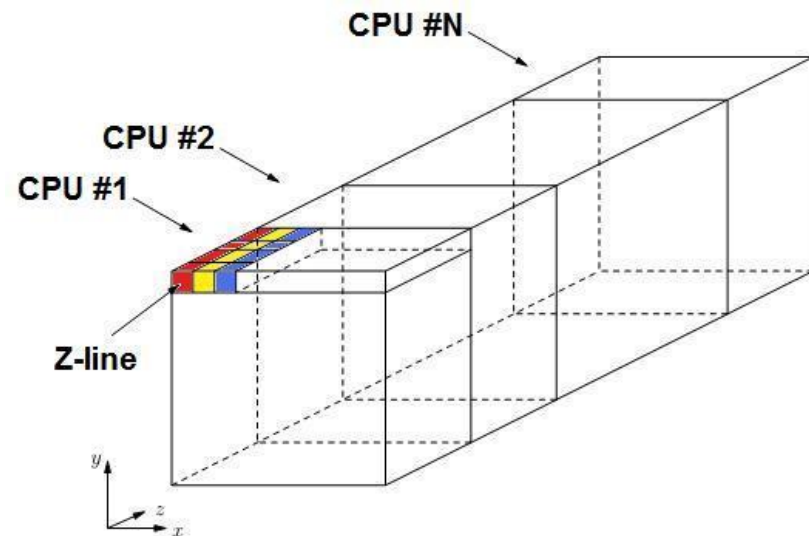
$$D_{ii} = \frac{1}{\text{noise variance}} = \frac{I_i^2}{I_i^2 + S_e^2} \approx I_i$$

- **MBIR uses information that FBP throws away!**

- Uses photon counts to estimate noise variance
- This results in a data dependent ill-conditioned optimization problem

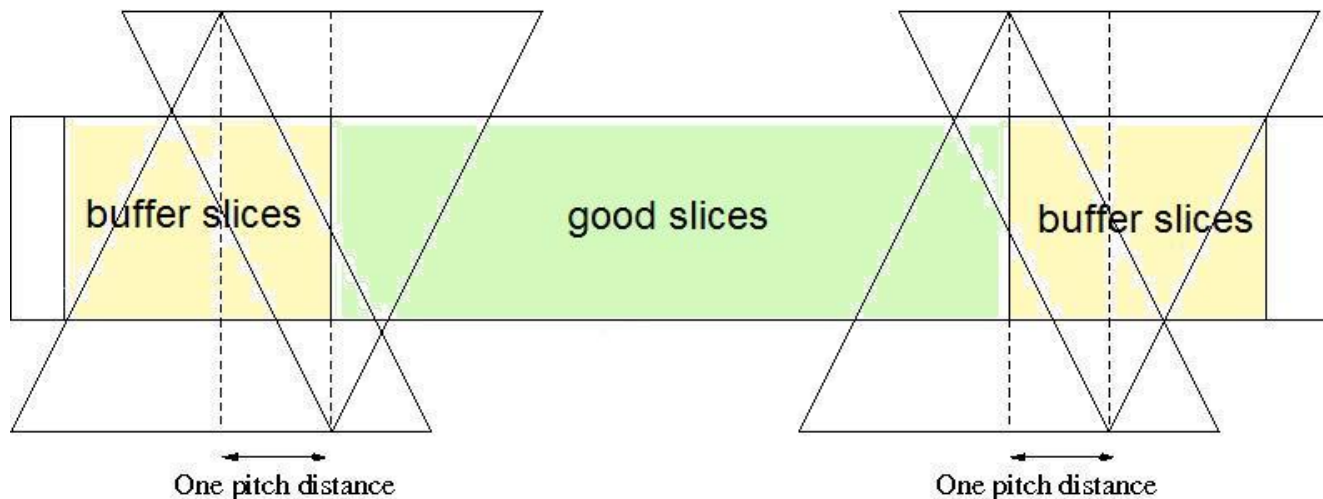
# Multi-Core Parallelization of ICD

- Implemented
  - Parallel ICD on 24 core shared memory Linux machine with p-threads
  - Speedup allows for fast algorithm development
- Performance issues
  - Computation tends to be limited by memory/caching speed, not computation
  - Memory must be organized as view, channel, row (slow to fast variables)
  - Allocation of slices to cores must balance computation/bandwidth load
- Architecture of parallel algorithm
  - Each core is responsible for updating voxels in a range of slices
  - Z-line updates:
    - A Z-line is a set of voxels along z, but at the same (x,y) position
    - Processors do ICD update along Z-lines
    - Leads to much better cash efficiency



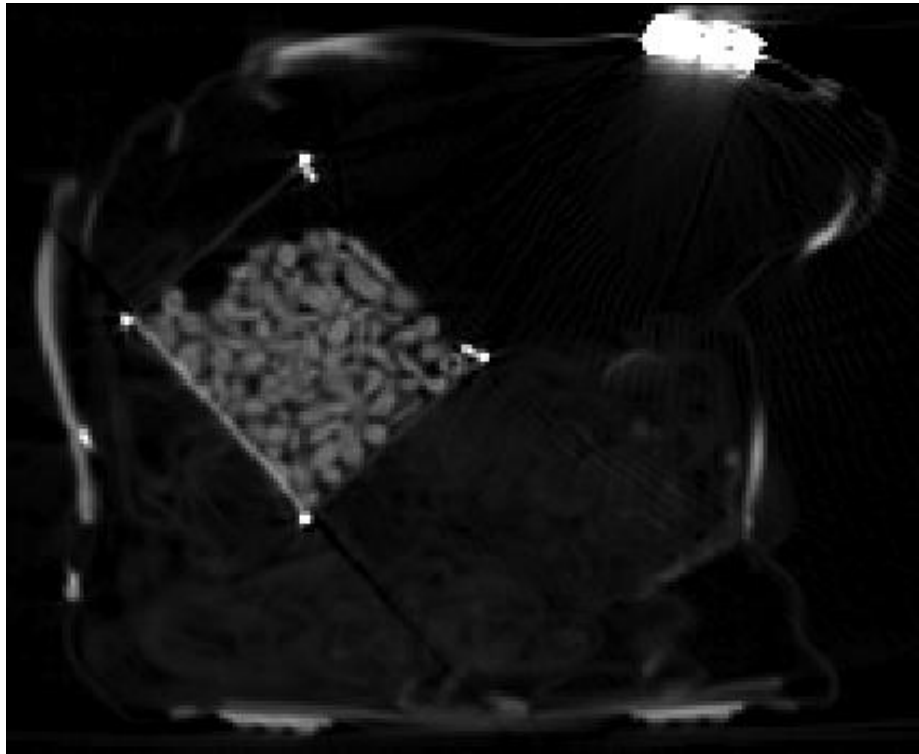
# Boundary condition and buffer slices

- For helical scan reconstructions, it is necessary to reconstruct buffer slices on both sides of the ROI
  - Buffer slices are discarded, but required for accurate reconstruction
  - Width of each set of buffer slices is approximately half the width of detector array
  - Computation associated with buffer slices is overhead

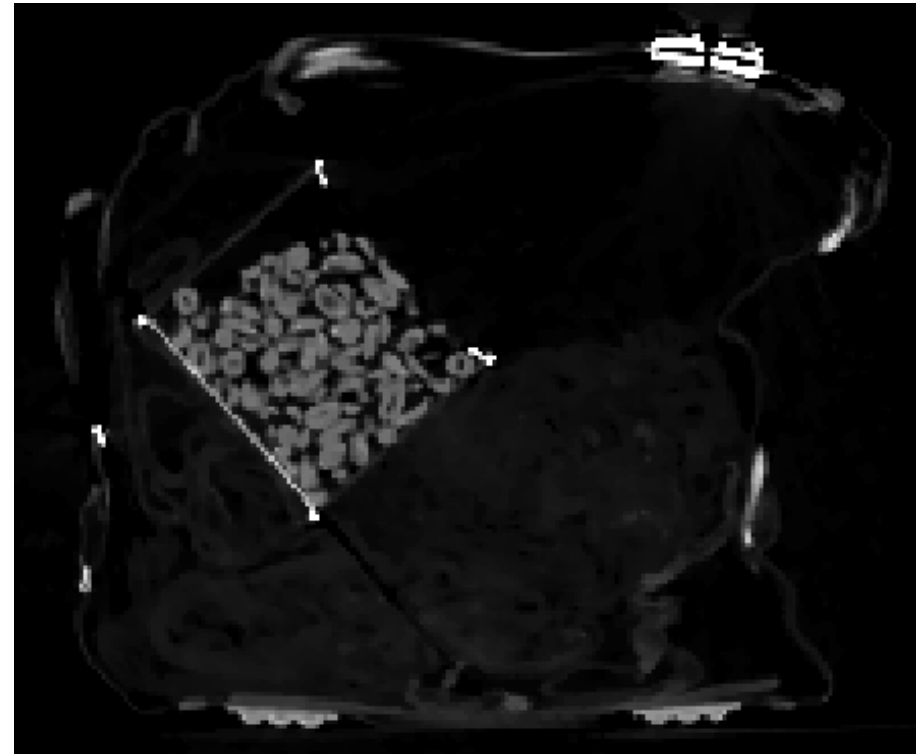


# Results: resolution and object discrimination

DFM

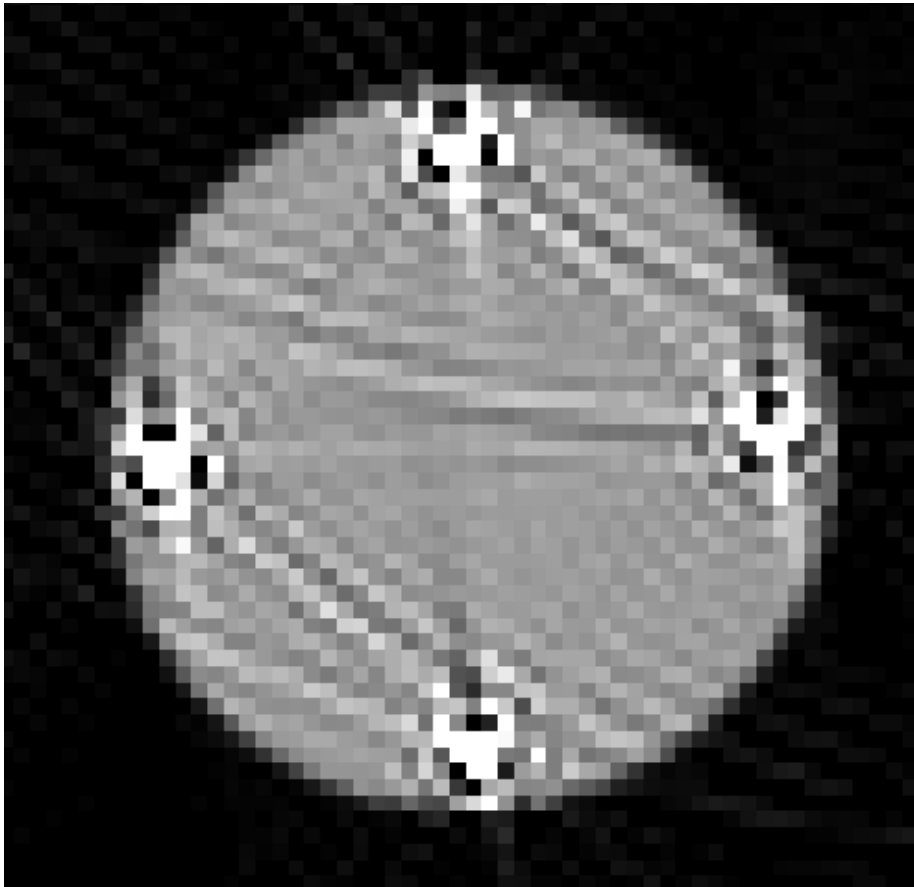


MBIR

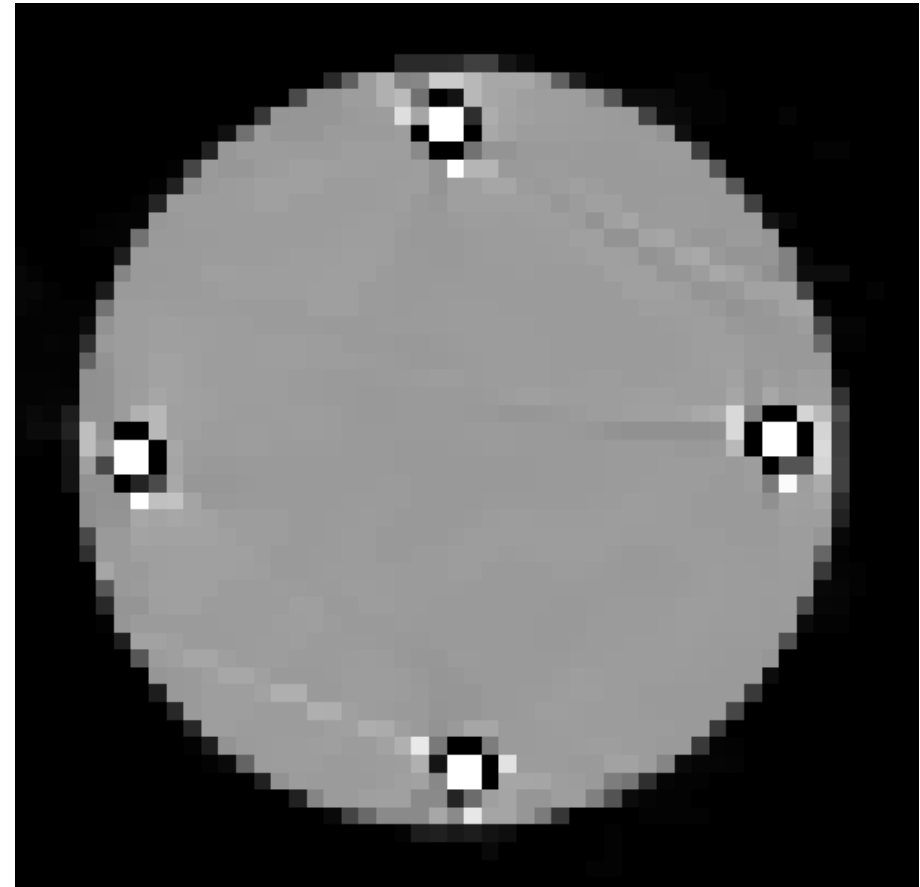


# Results: metal artifact reduction

DFM



MBIR





# Mixed power law data weighting

- Want to adjust the data weighting in the cost according to the suspected presence of metal in each projection measurement
- First using an initial reconstruction,  $x^{(0)}$ , define a metal indicator for each projection  $i$ ,

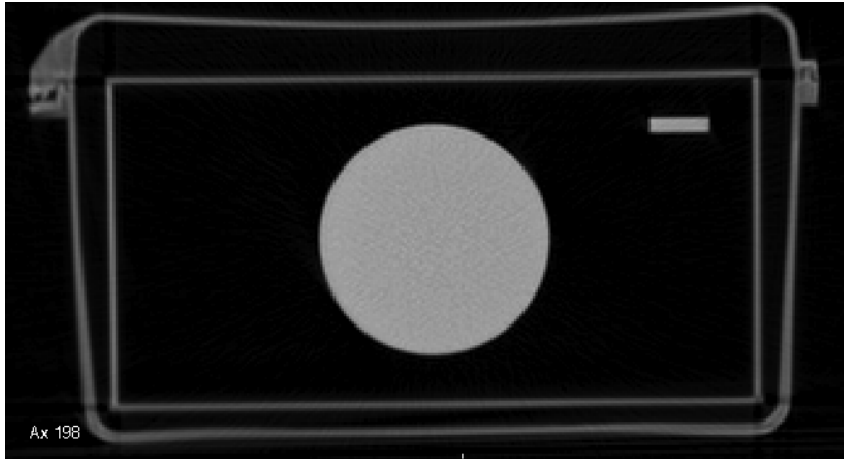
$$I_i = \begin{cases} 1, & \text{if for some voxel } j, \text{ both } A_{ij} > 0 \text{ and } x_j^{(0)} > T \\ 0, & \text{otherwise} \end{cases}$$

- Mixed data weighting:  $D_{ii} = I_i \left( I_i / I_{T,i} \right) + (1 - I_i) \left( I_i / I_{T,i} \right)^{0.5}$

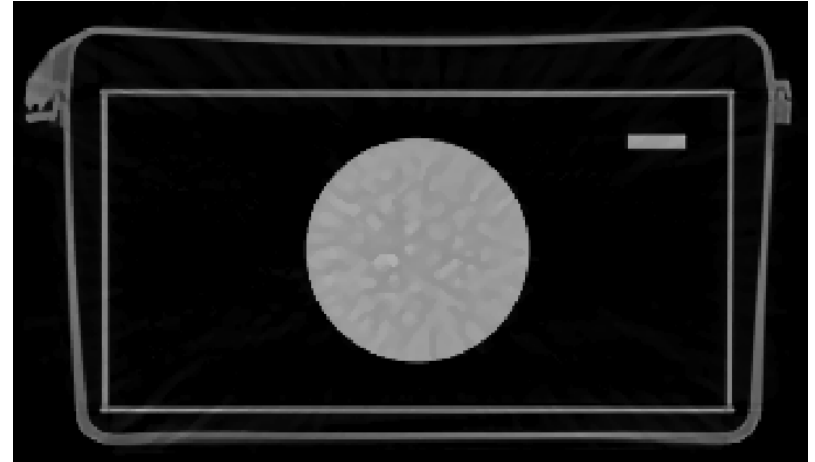
where  $I_i$  is the target scan count and  $I_{T,i}$  is the air scan count

# Results: power law data weighting

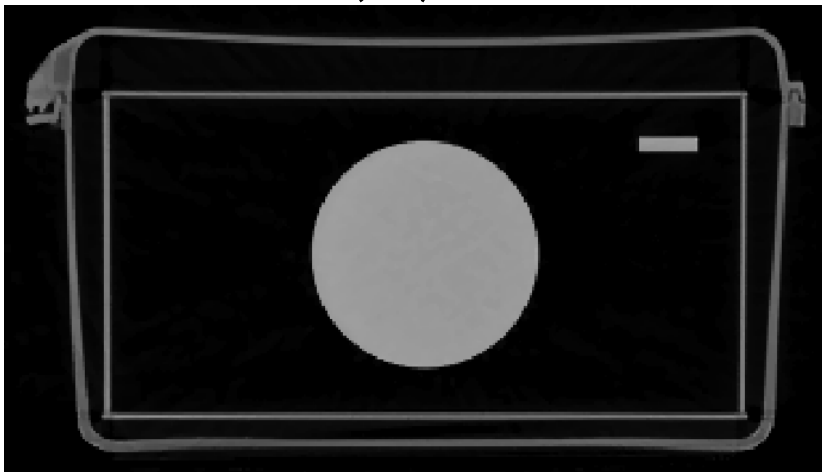
DFM



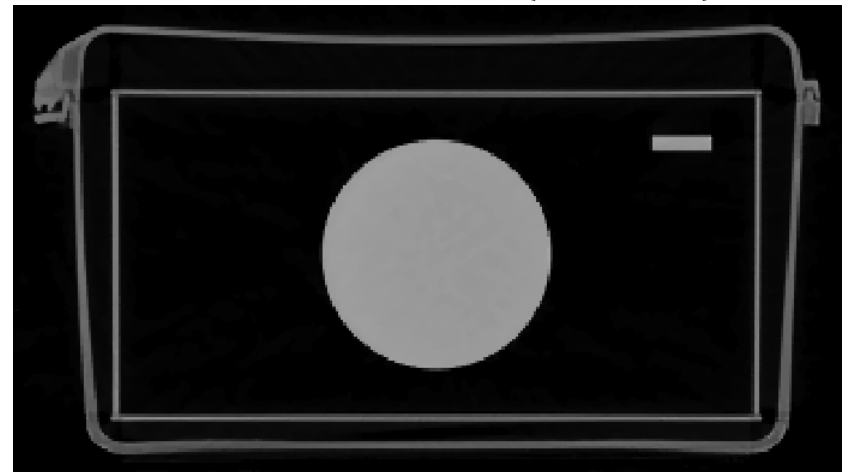
MBIR  $D_{ii} = I_i$



MBIR  $D_{ii} = (I_i)^{0.5}$

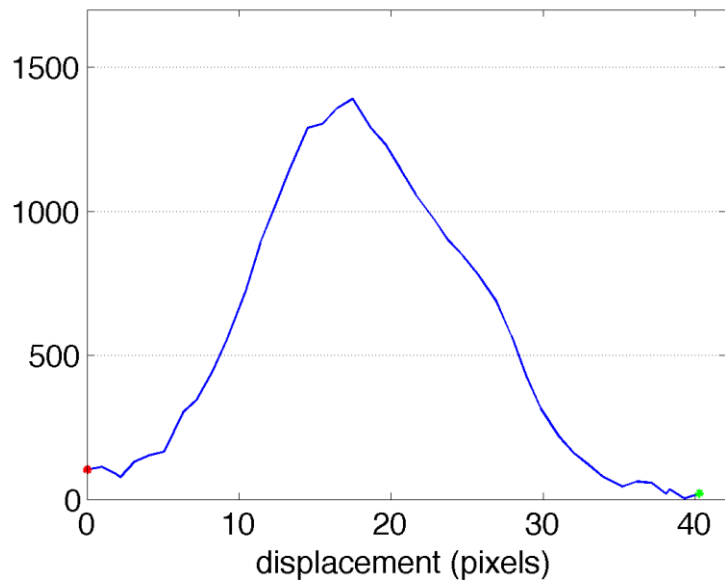


MBIR  $D_{ii} = \text{mixed} \{ I_i, I_i^{0.5} \}$

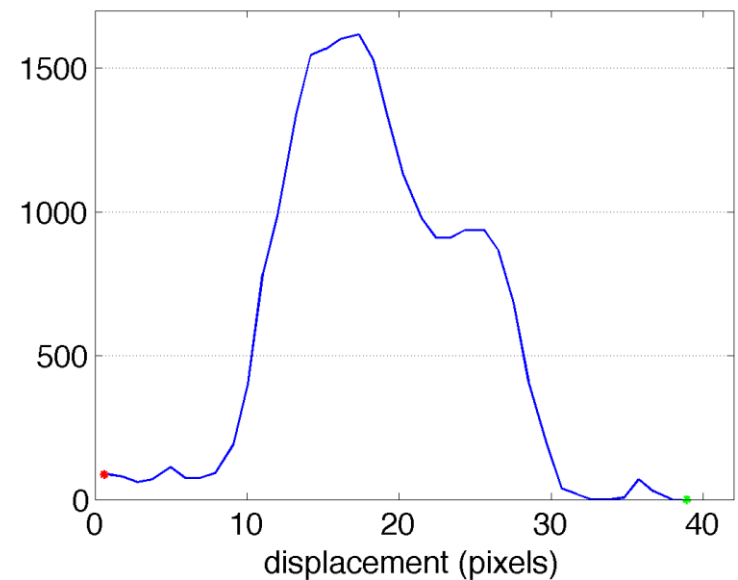
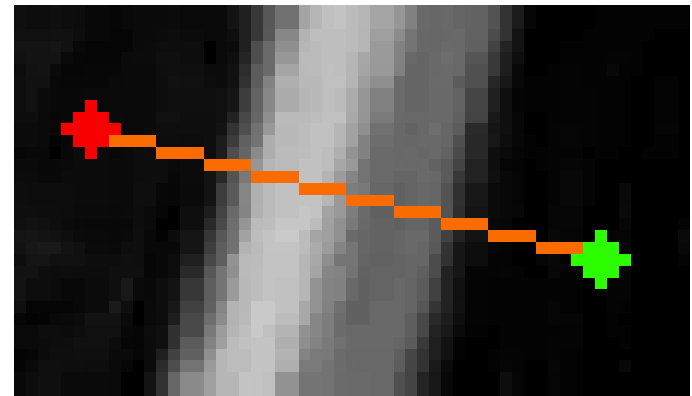


# Results: object discrimination

## DFM

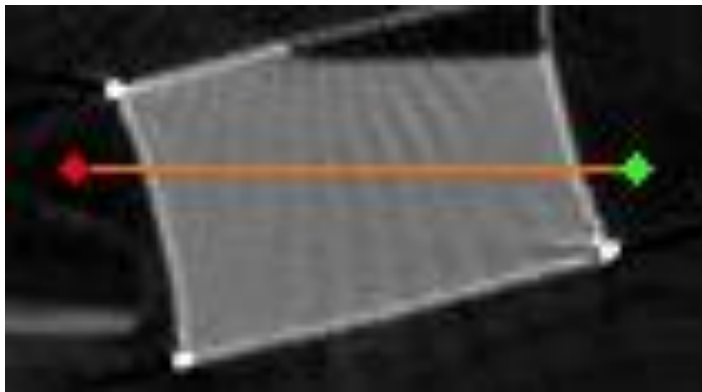


## MBIR

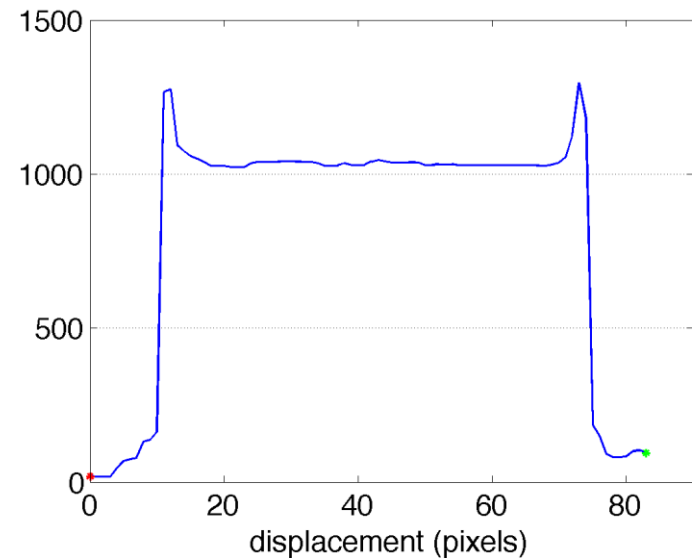
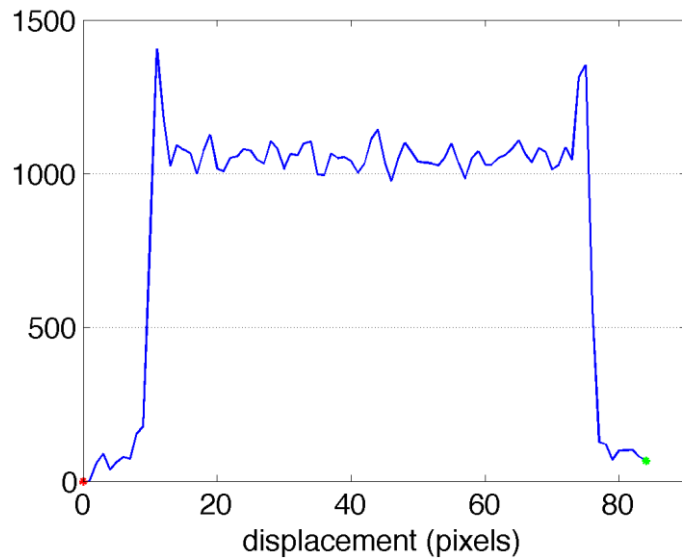
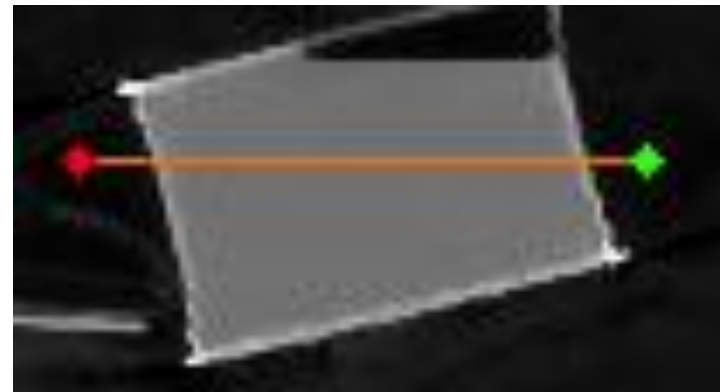


# Results: metal artifact reduction

## DFM

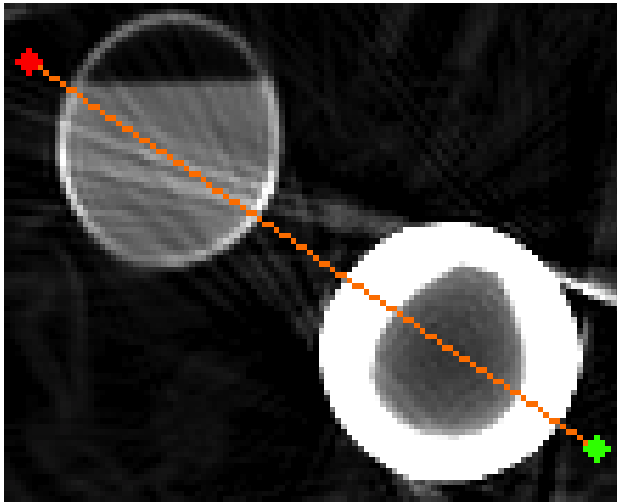


## MBIR

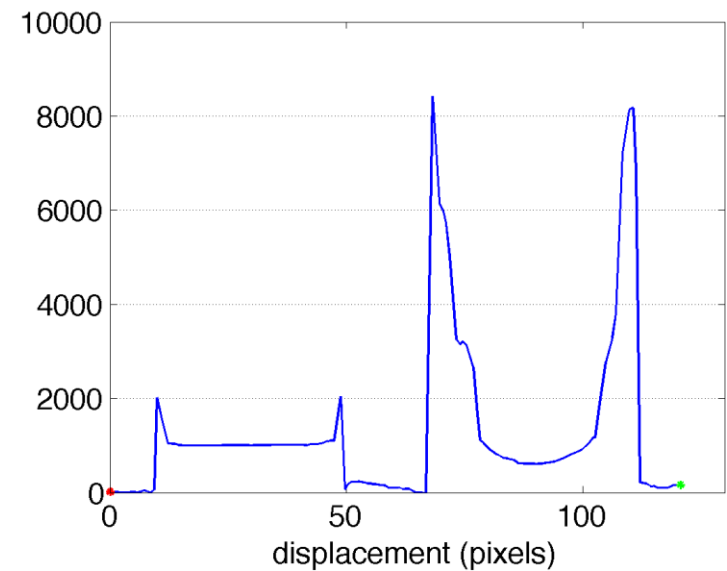
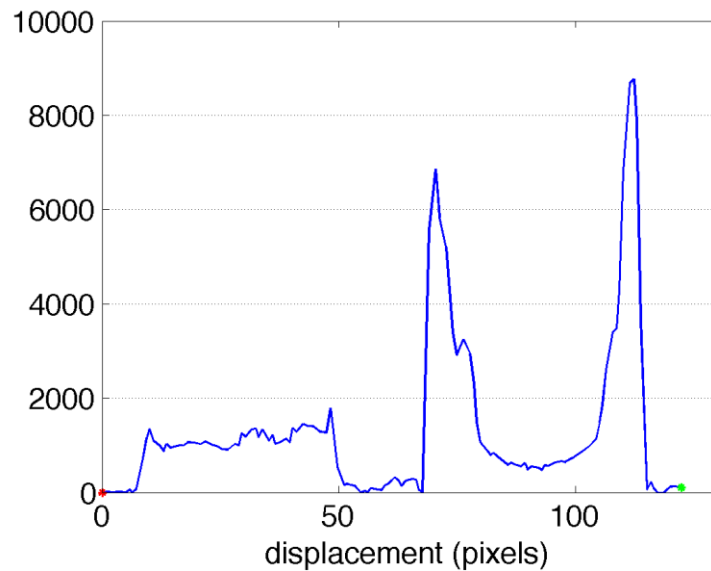
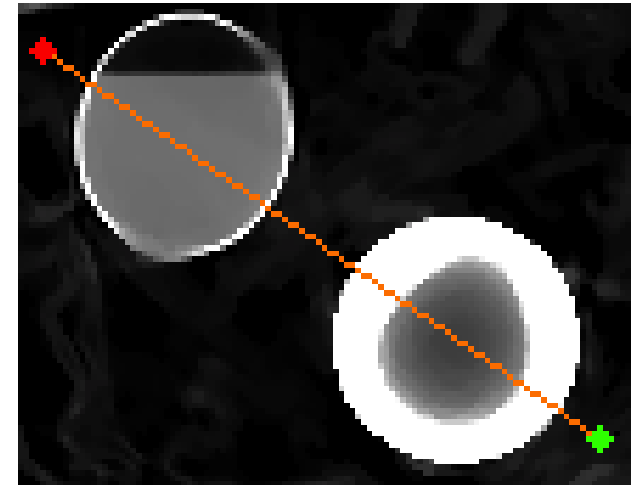


# Results: artifact reduction

DFM

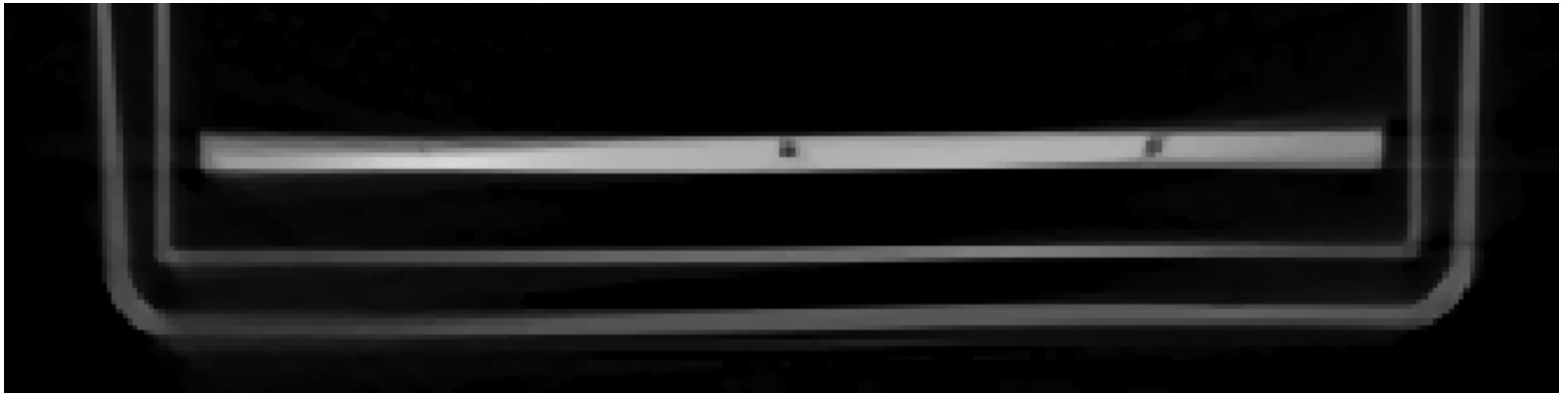


MBIR

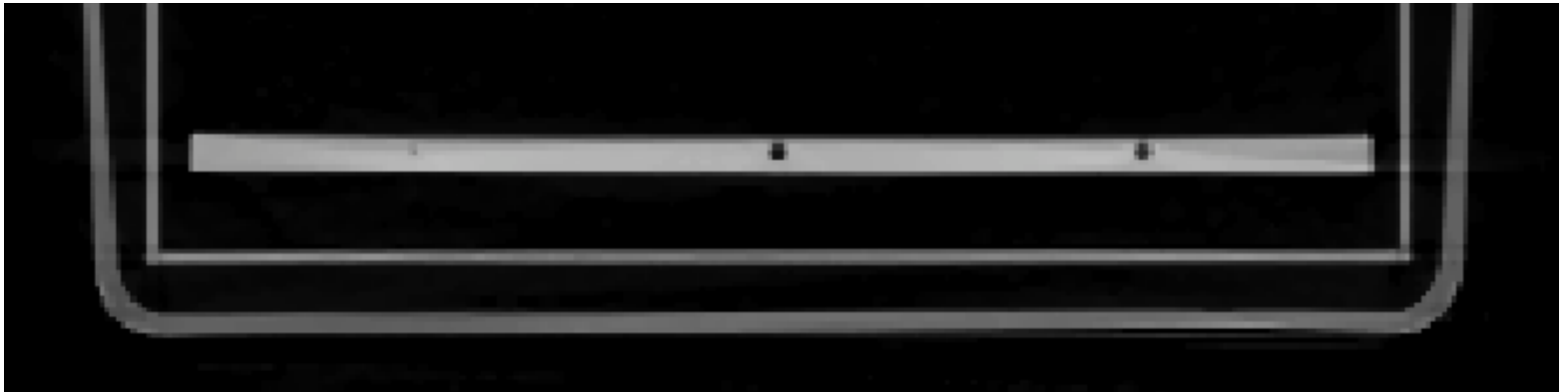


# Detector afterglow correction

before

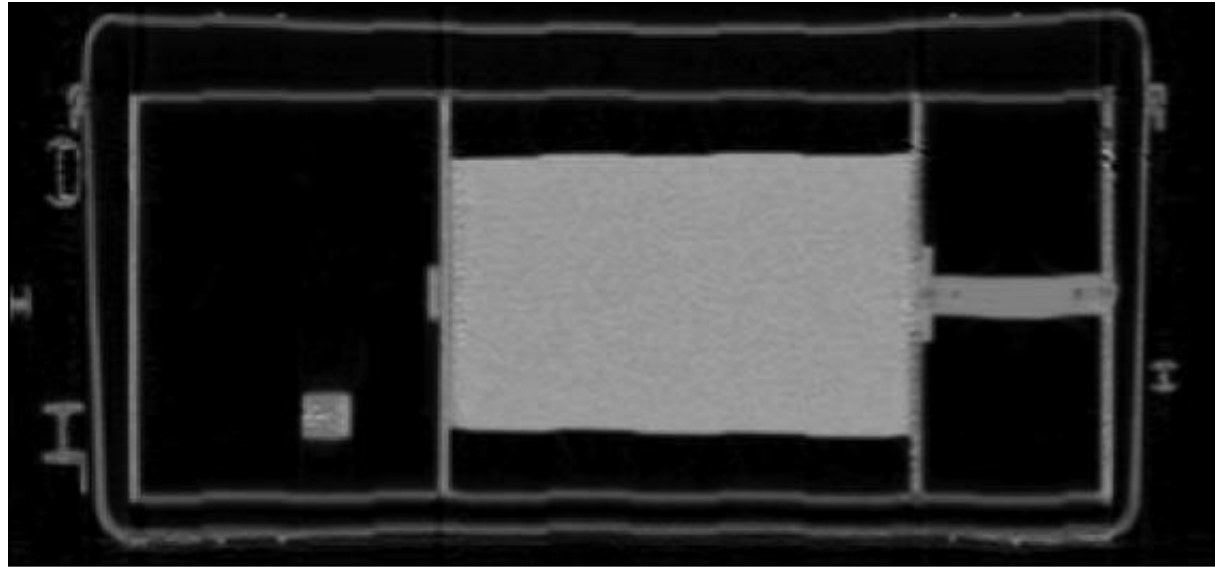


after

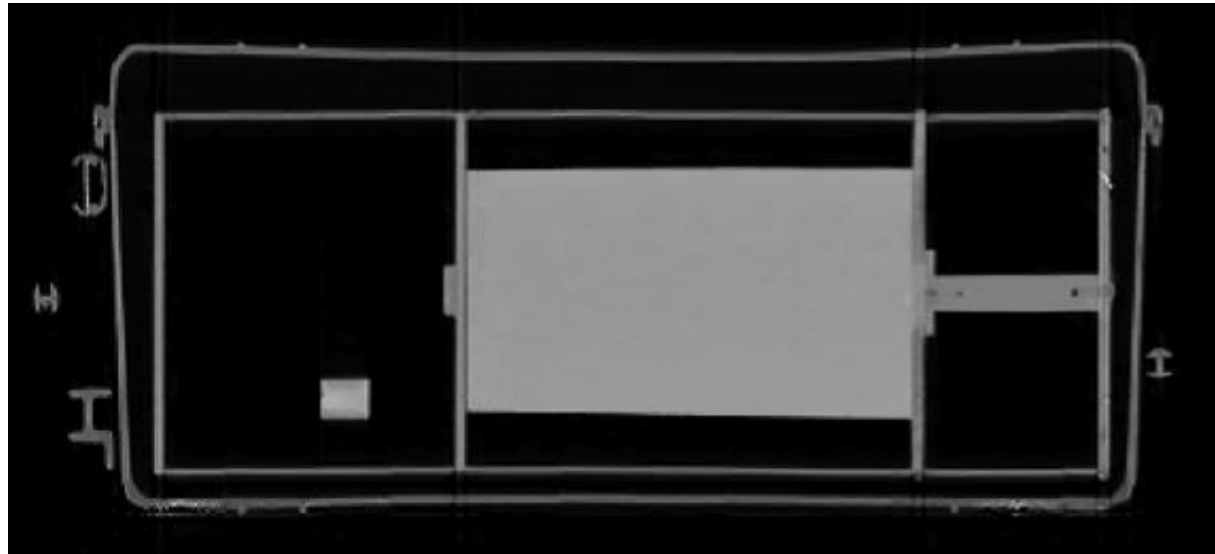


# Fan angle offset correction

DFM w/out  
correction



MBIR with  
correction



# Industry/University Collaboration

- My background:
  - 12 year GE relationship: *Veo* and 3T MRI
  - 20 years HP relationship: Technology in millions of printers
  - Signal Processing: Applied math, algorithms, physical models
- The opportunity:
  - Technology transfer from university to large company
  - Build on company's infrastructure
  - Provide university an efficient path to impact
- The obstacles:
  - Trust, IP, information sharing, risk
  - Understanding need to make money
  - Understanding need to publish and educate
- The keys to success:
  - Industry researcher who takes ownership
  - University researcher committed to success
  - Technology that will differentiate industry in the marketplace



# Summary

- MBIR offers great potential in baggage screening
  - Improved resolution
  - Reduced artifacts
  - Increased design flexibility
- Model accuracy is important
- Computation remains a challenge
  
- Key's to success in industry university partnership:
  - Trust
  - Committed team of researchers on both sides
  - Tight integration of research with clear goals

# MBIR/Veo Publications and Patents

- Some key publications:

K. Sauer and C. Bouman, "A Local Update Strategy for Iterative Reconstruction from Projections," *IEEE Trans. on Sig. Proc.*, vol. 41, no. 2, pp. 534-548, Feb. 1993.

C. A. Bouman and K. Sauer, "A Unified Approach to Statistical Tomography using Coordinate Descent Optimization," *IEEE Trans. on Image Processing*, vol. 5, no. 3, pp. 480-492, March 1996.

J.-B. Thibault, K. Sauer, C. Bouman, and J. Hsieh, "A Three-Dimensional Statistical Approach to Improved Image Quality for Multi-Slice Helical CT," *Medical Physics*, pp. 4526-4544, vol. 34, no. 11, November 2007.

- Issued patents:

1.J. Hsieh, J.-B. Thibault, C. A. Bouman, and K. Sauer, "An Iterative Method for Region-of-Interest Reconstruction," US Pat. 6,768,782, July 27, 2004.

2.9. K. Sauer, C. A. Bouman, J.-B. Thibault, and J. Hsieh, "Iterative Reconstruction Methods for Multi-Slice CT," US Pat. 6,907,102, June 14, 2005.

3.K. D. Sauer, J.-B. Thibault, C. A. Bouman, and J. Hsieh, "Methods, Apparatus, and Software to Facilitate Iterative Reconstruction of Images," US Pat. 7,251,306, July 31, 2007.

4.J.-B. Thibault, K. D. Sauer, C. A. Bouman, and J. Hsieh, "Methods, Apparatus, and Software to Facilitate Computing the Elements of a Forward Projection Matrix," US Pat. 7,272,205, Sep. 18, 2007.

5.C. A. Bouman, K. D. Sauer, J. Hsieh, and J.-B. Thibault, "Methods, Apparatus, and Software for Reconstructing an Image," US Pat. 7,308,071, Dec. 11, 2007.

6.K. D. Sauer, J.-B. Thibault, C. A. Bouman, and J. Hsieh, "Method, Apparatus, and Software for Reconstructing an Image," US Pat. 7,327,822, Feb. 5, 2008.

7.J. Hsieh, C. A. Bouman, K. D. Sauer, and J.-B. Thibault, "Methods, Apparatus, and Software for Failed or Degraded Components," US Pat. 7,440,602, Oct. 21, 2008.

8.J. Hsieh, J.-B. Thibault, K. D. Sauer, and C. A. Bouman, "Method and System for Improving a Resolution of an Image," US Pat. 7,583,780, Sept. 1, 2009.

9.K. D. Sauer, C. A. Bouman, J. Hsieh, and J.-B. Thibault, "Systems and Methods for Filtering Data in Medical Imaging Systems," US Pat. 7,676,074, Mar. 9, 2010.

10.K. D. Sauer, C. A. Bouman, J. Hsieh, and J.-B. Thibault, "Method and System for Image Reconstruction," US Pat. 7,885,371, Feb. 8, 2011.

11.K. D. Sauer, C. A. Bouman, J. Hsieh, and J.-B. Thibault, "Methods and Systems for Improving Quality of an Image," United States Patent 7,983,462. July 19, 2011.

12.Charles A. Bouman, Ken D. Sauer, Jean-Baptiste Thibault, and Zhou Yu, "Methods and System for Image Reconstruction," United States Patent 8,135,186. March 13, 2012.

13.Jean-Baptiste Thibault, Jiang Hsieh, Bruno De Man, Samit Basu, Zhou Yu, C. A. Bouman, Ken D. Sauer, "Method and System for Iterative Reconstruction," United States Patent 8,175,115. May 8, 2012.

14.Jiang Hsieh, Charles A. Bouman, Ken D. Sauer, and Jean-Baptiste Thibault, "Methods and Systems to Facilitate Correcting Gain Fluctuations in Image Reconstruction," United States Patent 8,218,715. July 10, 2012.

15.Jeffery A. Fessler, Charles A. Bouman, Jiang Hsieh, Jean-Baptiste D. M. Thibault, Ken D. Sauer, Samit K. Basu, and Bruno K. B. DeMan, "Methods and Systems for Improving Spatial and Temporal Resolution of Computed Images of Moving Objects," United States Patent 8,233,682. July 31, 2012.

# Distance-Driven (DD) forward projector

- CT forward projection is modeled by a linear matrix operation.

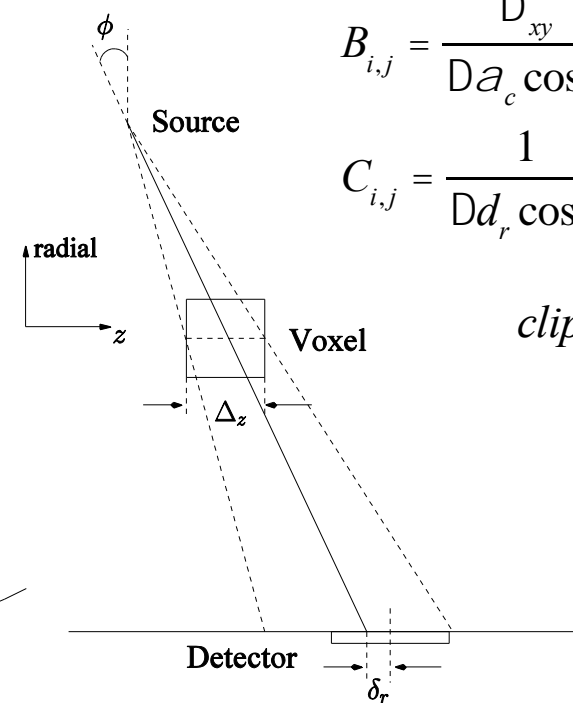
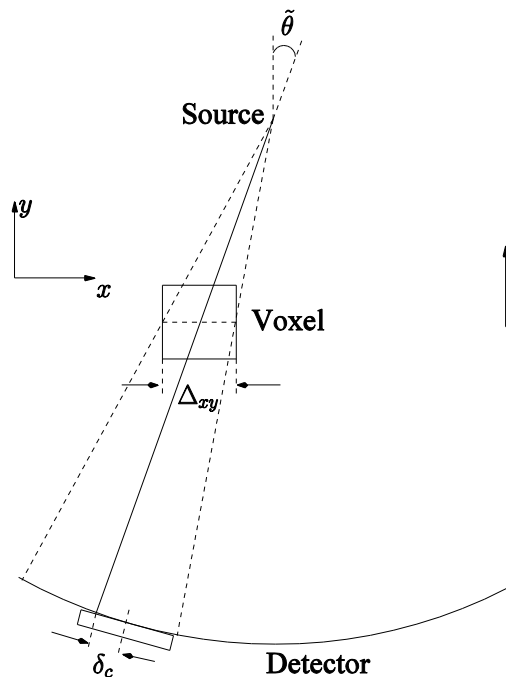
$$\begin{array}{c} \text{Sinogram} \\ \text{(Projection)} \end{array} \longrightarrow \begin{bmatrix} y \end{bmatrix} = \begin{bmatrix} A \end{bmatrix} \begin{bmatrix} x \end{bmatrix} \longleftarrow \text{Image voxels}$$

- The  $j$ -th column of  $A$  corresponds to projection of voxel  $j$ .
- In DD model, each voxel is flattened along the dimensions parallel to detector face.
- Each column entry is calculated as a product of XY-plane projection  $B_{i,j}$ , and Z-direction adjustment factor  $C_{i,j}$  for  $i$ -th detector element.

$$A_{i,j} = B_{i,j} \cdot C_{i,j}$$

# DD forward projector calculation

- The forward projection matrix  $A$  is calculated as  $A_{i,j} = B_{i,j} \cdot C_{i,j}$



$$B_{i,j} = \frac{D_{xy}}{Da_c \cos \tilde{q}} \text{clip} \left[ 0, \frac{W_c + Da_c}{2} - |d_c|, \min(W_c, Da_c) \right]$$

$$C_{i,j} = \frac{1}{Dd_r \cos f} \text{clip} \left[ 0, \frac{W_r + Dd_r}{2} - |d_r|, \min(W_r, Dd_r) \right]$$

$$\text{clip}[a, b, c] = \min(\max(a, b), c)$$

$D_{xy}$  : Voxel size

$\tilde{q}, f$  : Ray angle in XY-plane and Z-direction

$d_c, d_r$  : Offset from detector element center

$W_c, W_r$  : voxel projection width in channel and row directions

$Da_c, Dd_r$  : Detector width in channel and row directions

XY-plane

Z-direction

# Poisson noise model

- Use a 2<sup>nd</sup> order Taylor series expansion of true log likelihood

$$\log p(y|x) = - \sum_{i=1}^M \left( \frac{y_i}{l_{0,i}} \exp(-A_{i,*}x) + l_i A_{i,*}x + \log(l_i!) - l_i \log(l_{0,i}) \right)$$

$$\gg -\frac{1}{2} (y - Ax)^t D (y - Ax) + c(l)$$

where

$$A_{i,*} = i^{th} \text{ row of } A$$

$$y_i = \log \left( \frac{l_{0,i}}{l_i} \right)$$

$$D_{i,i} = l_i$$

- $A$  - forward system matrix
- $D$  - diagonal weighting matrix

# Iterative Coordinate Descent (ICD)

- Iteratively match each pixel (i.e. each column of  $A$ )
- Select each pixel to minimize total cost

$$p_i = A_{*,j} x_j$$

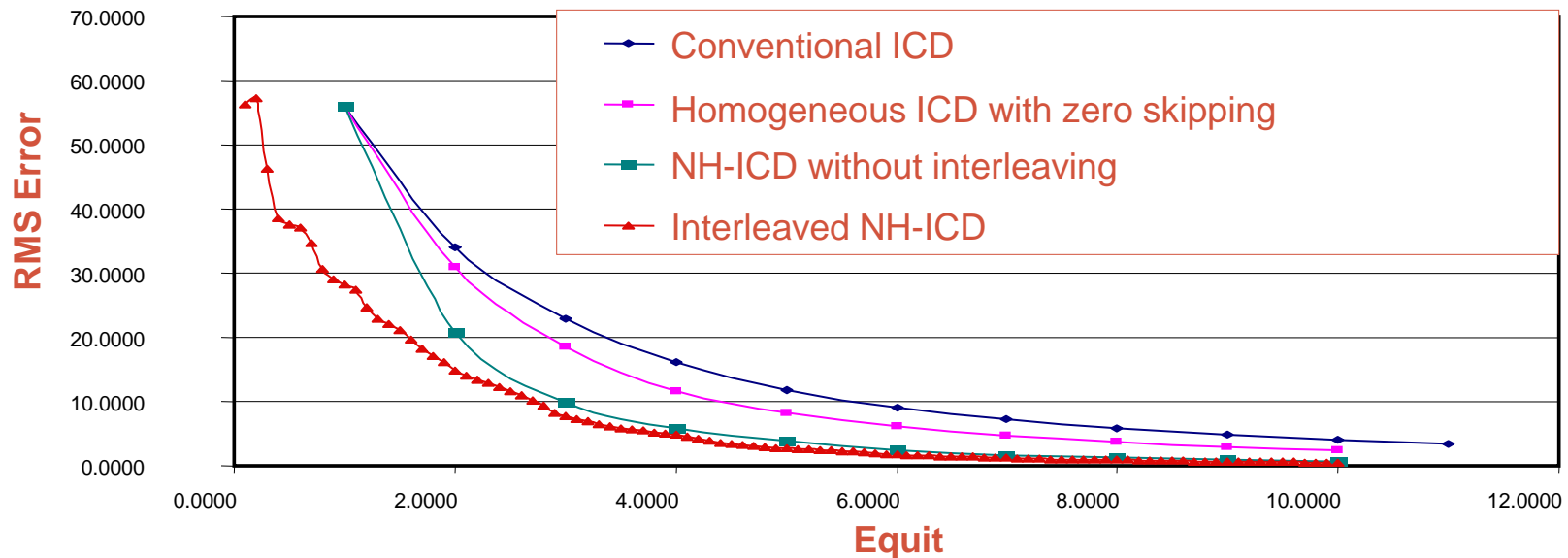
$$x_j \leftarrow \arg \min_{x_j} \left\{ \frac{1}{2} \|y - Ax\|_L^2 + U(x) \right\}$$

- Issues:
  - Efficient update by using sinogram error state
  - High spatial frequencies converge first
  - Benefits from good initial condition

# Why ICD ?

- **Advantages:**
  - Fast convergence at high spatial frequencies
  - Can be initialized with FBP
  - Sequence of 1D updates provides flexibility
  - Easy to enforce positivity constraints
  - Robust to non-idealities
- **Disadvantages**
  - Poor low frequency convergence
  - Irregular memory access

# RMSE Convergence Plots for NH-ICD

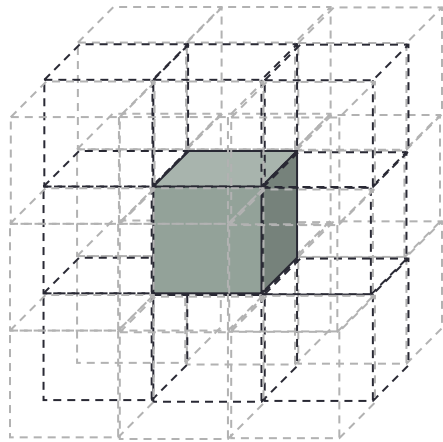


- NH-ICD

- Reduces transients at early stage allowing faster convergence
- Interleaving in early iterations further improves convergence speed



# Image prior model



$$U(\mathbf{x}) = \frac{1}{pS^p} \sum_{\{j,k\} \in C} r(x_j - x_k)$$

$$r(D) = |D| \quad \text{Total Variation/Compressed Sensing}$$

$$r(D) = |D|^p \quad \text{Generalized Gaussian MRF}$$

where  $p = 1.2$

$$r(D) = \frac{|D|^q}{1 + |D/50|^{q-p}} \quad \text{Q-GGMRF}$$

with  $p = 1.2$  and  $q = 2$

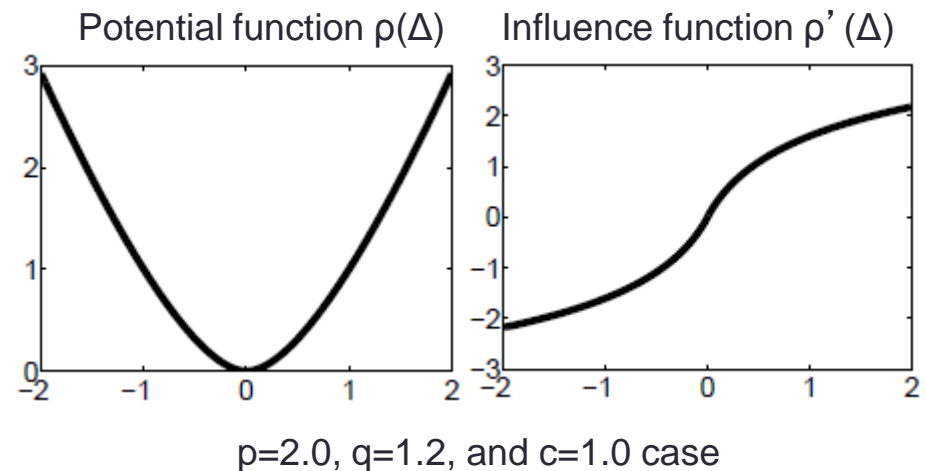
- 3D regularization using 26 neighbors
- Design to:
  - Preserve high contrast edges
  - Enhance low contrast sensitivity

# Prior: Q-Generalized Gaussian MRF

- Define neighboring pixel difference  $\Delta = x_s - x_r$ . The q-GGMRF prior is defined as

$$p(x) = \frac{1}{z} \exp \left\{ -\frac{1}{q\sigma_x^q} \sum_{\{s,r\} \in \mathcal{C}} g_{s,r} \rho(\Delta) \right\}$$

$$\text{where } \rho(\Delta) = \frac{|\Delta|^p}{1 + \left| \frac{\Delta}{c} \right|^{p-q}}$$

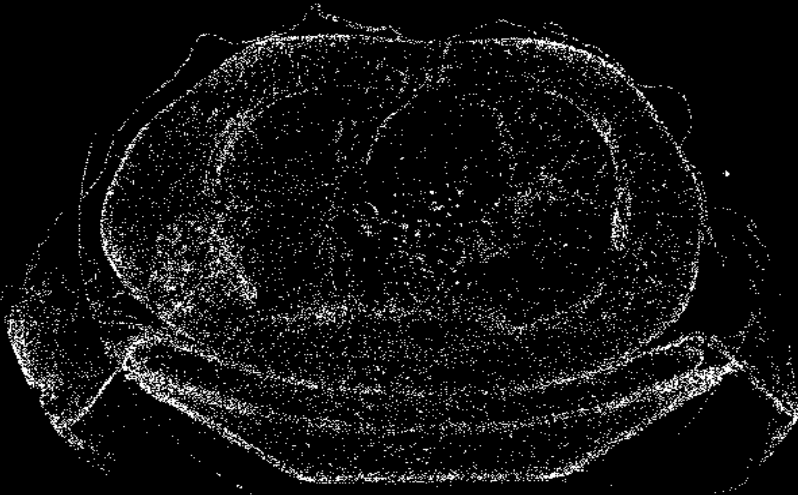


- Controls both low and high-contrast behavior
- Parameter  $c$  is a soft transition point such that  $r(D) \approx \begin{cases} |D|^p & \text{for } |D| \ll c \\ |D|^q & \text{for } |D| \gg c \end{cases}$
- Gaussian MRF (GMRF) prior is the special case where  $p=q=2$ , i.e.  $r(D) = D^2$

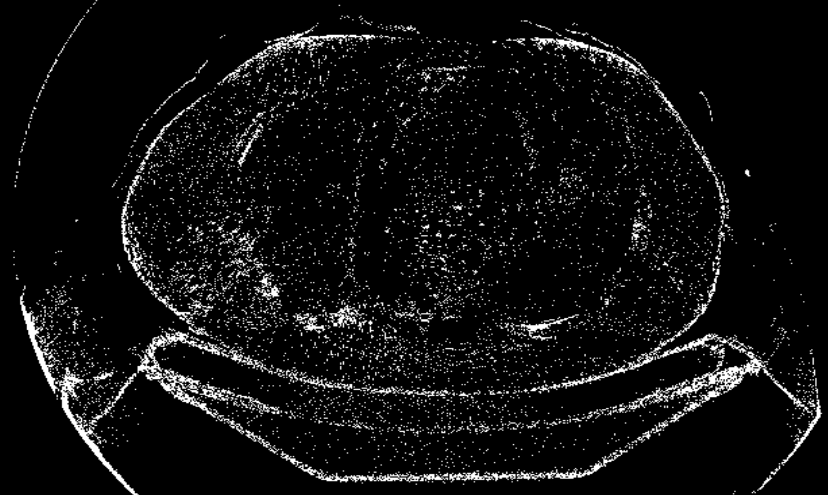
# Non-Homogeneous ICD (NHICD)

- Objective: find good correlation between update map and true RMS error at different stages of

Top 5% pixels with largest  
update values at iteration 1



Top 5% pixels with largest  
RMS error at iteration 1



# Model-Based Iterative Reconstruction

- Our framework is the *maximum a posteriori* (MAP) estimate

$$\hat{x}_{MAP} = \arg \max_{x \geq 0} \left\{ \overbrace{\log p(y | x)}^{\text{Data term}} + \overbrace{\log p(x)}^{\text{Prior term}} \right\}$$

- Vector  $y$  is the projection measurements, and  $x$  is the image
- MBIR is used in GE Healthcare's Veo product which is sold in US and European markets since 11/2011
- We are working with Morpho Detection to investigate the use of MBIR in an EDS system for aviation security

# Evaluation for EDS performance

- Evaluated qualitative impact of model-based reconstructions on proprietary automatic threat detection (ATD) algorithms
  - Improved segmentation
  - Improved object identification/classification
  - Improved separation of adjoining objects
  - Reduction in false alarms
- In addition, the improvements in reconstruction quality provide for better operator experience
- Reduced cost of additional detection